

## UNIVERSITY OF SOUTH FLORIDA

### *Beyond Photovoltaics: Nanoscale Rectenna for Conversion of Solar and Thermal Energy to Electricity*

**PI:** Shekhar Bhansali **Co-PI's:** Elias Stefanakos, Yogi Goswami, Subramanian Krishnan

**Students:** Rudran Ratnadurai, Electrical Engineering, Ph.D.

Michael Celestin, Chemical Engineering, Ph.D.

Samantha Wijewardane, Mechanical Engineering, Ph.D.

Justin Boone, Electrical Engineering, Ph.D.

**Description:** The main objective of the proposal is to commercialize and scale up a new technology, rectenna to convert waste heat energy to electricity. Although the prediction of highly efficient (~85%) solar rectennas was published almost 30 years ago, serious technological challenges have prevented such devices from becoming a reality. Since the ultimate goal of a direct optical frequency rectenna photovoltaic power converter is still likely a decade away, we plan to convert optical solar radiation to thermal radiation (~30 THz regime) using an innovative blackbody source. Leveraging the research efforts of the world-class team members, we plan to further develop the rectenna technology that is within reach of efficient radiation conversion at 30 THz. A fully integrated, blackbody converter and 30 THz rectenna system will be capable of converting at least 50% of solar and thermal energy into usable electrical power, clearly demonstrating a truly transformational new technology in the renewable energy technology sector.

**Budget:** \$598,500

**Universities:** USF

**External Collaborators:** Sandia Research Laboratory, University of New Mexico, Bhabha Atomic Research Center, India

## Progress Summary

### Objectives:

The research objective of this project is to develop a high efficiency solar/ thermal energy conversion using antenna coupled MIM tunnel junction. Towards this, the follow tasks were charted,

- Fabrication, characterization and testing of Metal-Insulator-Metal tunnel junction,
- Design, fabrication and testing of antenna,
- Integration of antenna and MIM junction.

### Approach:

- Evaluate the feasibility of using organic insulator in the fabrication of MIM junctions and develop a hybrid device for energy conversion
- Characterize the organic insulator layer to yield reliable electrical response
- Investigate the effect of different deposition parameters on the working of MIM junctions
- Evaluate different design configurations of the MIM junction and determine the most reliable and scalable nanomanufacturing process
- Investigate the design of a dual antenna design for rectenna application

### Accomplishments:

- Self-Aligned Monolayers that uses thiol chemistry such as dodecane and octadecanethiols were characterized using impedance spectroscopy to determine the thickness of the monolayers. Such monolayers were utilized to develop a hybrid MIM tunnel junction using e-beam and optical lithography.

- The roughness and thickness of the metal electrodes were modified for the thiols to have a better adhesion, hence yield better electrical characteristics.
- Nickel Oxide films were deposited under different reactive gas ratio and its effect on the electrical behavior of the junction was determined.
- Based on the most stable deposition parameters, MIM junctions with various configurations were fabricated and electrical response was determined.
- The antenna structure was designed to house a slot and dipole antenna to improve the return loss of the antenna.

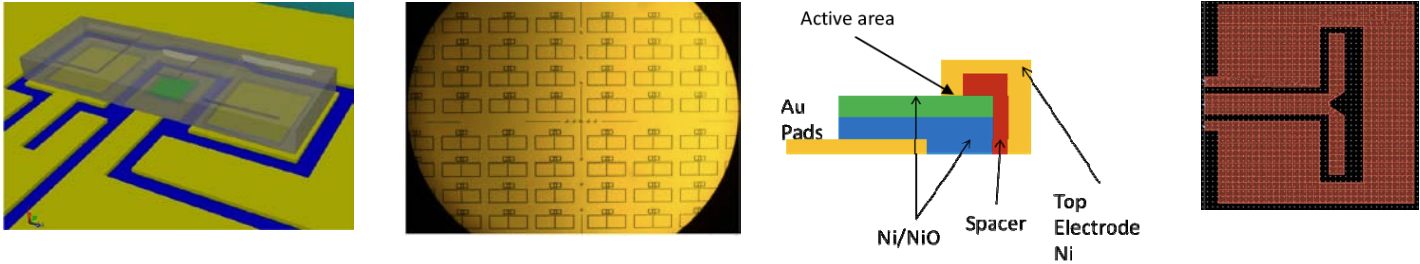


Figure 1: Micrograph images showing (a) schematic of MIM junction with a organic insulator, (b) fabricated organic MIM junction array, (c) schematic of a new constructed sidewall design and (d) redesigned antenna structure

## 2010 Annual Report

### Introduction:

Over the past three decades, there has been an exponential increase in demand for energy [1]. As the economies grow around the world, the increase in demand for energy will continue. While clean coal technologies are expected to supply a major share of energy, there is growing recognition of the benefits of renewable energy sources. The two major approaches to renewable energy in the past decade have been solar and wind. Solar energy has been demonstrated to be more stable source with smaller impact on environment. Although solar energy grid connectivity has grown in double digits over the past decade, its current install base (2010) is still under 0.5% of the world demand of energy. A simple approach to increasing the efficiency of solar/thermal energy installations would be to convert the waste heat into useful energy. The theoretical conversion of thermal energy into electrical energy using current approaches is limited by the Carnot cycle to between 30-40% based on starting temperatures. Exploiting the wave nature of the IR radiation using the rectenna has the potential to increase the theoretical conversion limits to upwards of 98%.

### Approach:

Based on the research objective, during the current reporting period of the project, the main focus was to characterize the tunnel junction with organic insulator and develop a dual mode antenna. The antenna structures were developed with a dipole coupled slot structure resonating at 94 GHz. The antenna was designed in a co-planar waveguide configuration, which enables the testing of antenna parameters using a ground-signal-ground wafer probes. As a preliminary approach, several organic films (self-assembled monolayers) were procured and characterized for the thickness uniformity using impedance spectroscopy technique. 1-dodecanethiol was used as the insulator layer due to its better uniformity, control and thickness. A novel processing scheme was used, which incorporates e-beam lithography to define small contact areas. MIM tunnel junctions were fabricated with Au-SAM-Cr. In order to provide better electrical behavior, the SAM layer was optimized to yield maximum uniformity. Furthermore, the MIM

junctions fabricated with inorganic insulator layer using Ni-NiO-Cr were investigated for its electrical characteristics by varying the dielectric deposition condition. Specifically, the gas ratio used for depositing the inorganic insulator layer was varied and its effect on electrical behavior of the junction was determined. Based on the most stable insulator deposition parameters, the MIM junctions with various configurations were fabricated. The variance in current density from device to device was used as a comparative measure to determine the stable configuration and manufacturing technique

## Research Accomplishments

### (a) Evaluation of organic insulator as the dielectric in MIM tunnel junction

High frequency MIM junctions have been typically developed using solid-state materials. In this research task, MIM junctions have been developed with SAM films. Several alkanethiols were procured and a thiol with smallest chain length was used for junction development. Specifically, 1-dodecanethiol (DDT) was used as the organic dielectric. The devices have been fabricated on a silicon substrate through photolithography and E-beam lithography (EBL). Fig. 2 shows the schematic of the SAM MIM junction design.

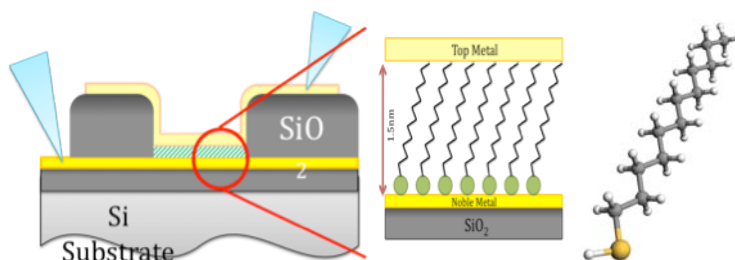


**Figure 2: A Schematic representation of the SAM based MIM tunnel junction**

Initially, a ground plane metal (gold) was deposited and patterned to form the bottom electrode as well as the contact pad for electrical testing. Then a window was patterned using EBL to deposit the thiol. A 1 mM solution of 1-Dodecanethiol was created in ethanol and the sample was immersion coated in the pre-opened window. A metal layer was deposited on top of the SAM layer to form a MIM structure. Fig. 3(a) shows an electron micrograph of the fabricated SAM array.

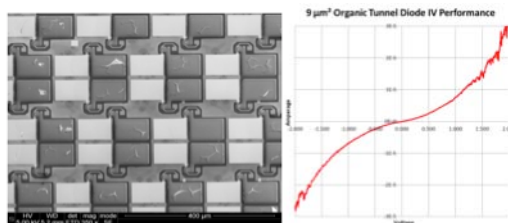


**Figure 3: Freshly evaporated Gold film on SAM structure and I-V from organic diode**

The I-V characteristic of the MIM tunnel junction fabricated with Au-SAM-Cr is shown in Fig 3(b). The SAM tunnel junctions exhibited low current with a slight asymmetry. The junctions exhibited highly non-linear I-V characteristics, required for rectification. Similar to the metal-oxide tunnel junctions, the SAM-based MIMs also exhibited very low current at low voltages, like square law-detectors and then exhibited an exponential curve. The resistance of these tunnel junctions was also similar to the solid-state tunnel junctions, typically in the range of a few kΩ. However, the junctions were more stable even at higher bias voltages, compared to the metal-oxide junctions. This is due to the thickness and homogeneity of the film. Thus from the electrical behavior of the SAM diode it can be stated that, although the asymmetry is not very significant, the resistance of the junctions is lesser than its metal-oxide counterpart, making it suitable for energy conversion and detection application. Results from the test probe setup revealed the current-voltage (IV) performance of the tunnel diode. There were a number of different sized junctions fabricated however the 9 μm<sup>2</sup> junctions offered the greatest yield. Smaller junctions would often be damaged due to fabrication errors and lithography exposure variations. This resulted in many open circuits, which did not allow current to pass. Much larger devices often experienced shorting (high current resistor performance) due to numerous grain defects in the film. While it is appealing to think of this self-assembled film as a perfect structure, it does contain a number of common defects resulting from monolayer collapse, grain boundaries, and substrate imperfections. As

reported by other groups, device yield at this optimum junction size was approximately 5%. For this configuration, the similar work functions of the opposing metals resulted in a highly symmetrical curve with little rectification performance. The tuned work function effects due to a film dipole are responsible for this result. Still, the signal output could be measured and the device used in a sensing application. Exploration of and SAMs with varied termination chemistry and other compatible metals, which can be evaporated at relatively low temperature, will yield better rectification performance.

### (b) Characterization of Self-Assembled Monolayer

1-Dodecanethiol >98% (DDT) and 200 proof ethanol were obtained from Sigma-Aldrich and used as received without further purification. A micropipette was used to meter DDT into 30mL of ethanol. This 1 mM solution was formed in a specially cleaned glass jar and mixed for 3 minutes in an ultrasonic bath. Samples were cleaned in oxygen plasma at 50 Watts for 2 minutes and immersed in the SAM solution within 10s of removal from the plasma. The glass jar was immediately purged with Argon and protected from light. The samples remained immersed for 36 hours when they were removed and rinsed in reagent alcohol, DI water, NanoPure water, and finally dried in an Argon stream.

The thickness of the SAM dielectric layer was determined using impedance spectroscopy. Results of the experiment are shown in Fig. 4. The slope is placed into Equation 1 and solved for a d value of 1.54nm.

$$\text{Slope}(0.0145) = (n^2 F^2 k_s / RT) e^{-\beta d} \quad (1)$$

This is in good agreement with the ArgusLab modeled chemical structure, which predicted a chain length of 16.31Å shown in Fig. 2. The reason the modeled molecule appears longer is because of the angle of tilt known to exist for Gold substrate grown SAMs. The exact angle varies by coordinating metal; in the case of Gold, the tilt angle is around 30°. Additionally, while the carbon chain was modeled as a fully extended trans-configuration structure, there will be a few chains around grain boundaries and defects, which contain folds and thus will

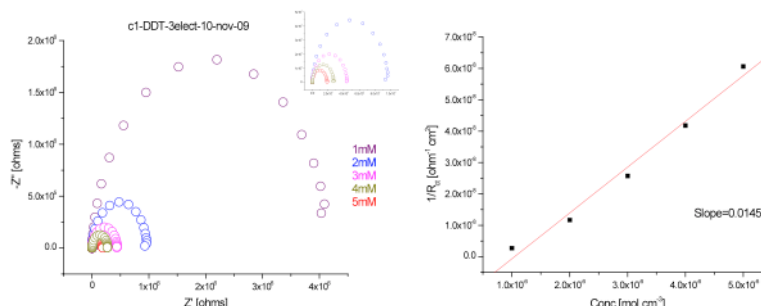


**Fig. 4. (a) Electrochemical impedance Nyquist diagram for 1-Dodecanethiol; (b) Dependence of reciprocal of the apparent resistance on conc.**

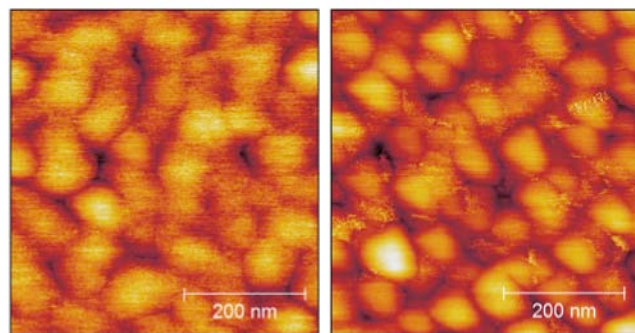


**Figure 5: AFM micrograph of gold layer with and without SAM**

appear shorter under analysis. Van der Waals interactions between neighboring chains strengthen the surface film—these effects are most prominent in chains of greater than 6 carbons in length. Atomic Force Microscope (AFM) analysis of the coated noble metal substrate revealed a change in roughness. Small Gold lattice defects and grains are masked by the tail ends of self-assembled film as seen between Fig. 5(a) and (b). In the case of non-terminated carbon chains as seen here, the tail ends are very small and offer poor contrast for individual view by AFM.

**(b) Effect of varying the dielectric deposition condition**

The critical factor that aids the fast switching nature of the MIM tunnel junction are (a) the thickness of the insulator and (b) the interface condition. In order to facilitate energy conversion, the insulator layer of the MIM junctions needs to be thin (~1-3nm) and homogenous. Numerous studies have been done on the characterization of MIM junction based on the insulator thickness and metal contact area. However, the effect of varying the insulator deposition condition on the working of MIM diode is yet to be determined. In this research, Nickel Oxide was deposited under different Ar:O<sub>2</sub> gas concentration to quantify the effect of deposition condition on the electrical characteristics of the tunnel junction, specifically the gas ratios used were 1:1, 1:2 and 1:3. Thus by using the deposition conditions as the control parameter, the electrical behavior and the nature of the insulator layer were determined.

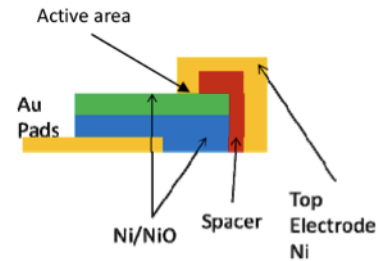


**Figure 6: A schematic of the stacked MIM configuration with isolation layer**

MIM junctions were fabricated using Ni-NiO-Cr using a stacked configuration as shown in Fig.7. In this configuration an isolation layer was used to avoid any potential sidewall contact with the top electrode. It also prevents improper insulator coverage in the sidewalls. Fig 7 (a-c) show the I-V responses of the devices. Ten consecutive measurements were performed on the device on each substrate to prevent inaccurate measurements due to surface or trapped charges. As can be seen, fig. 7(a) and 7(c) show similar current outputs. Substrate A(1:1) exhibits around 15µA at 600m and substrate C(1:3) exhibits twice as much. It can be inferred that along with thermionic tunnelling and Fowler Nordheim (F-N) tunnelling, insulator layers with excess of O<sub>2</sub> and those with deficient O<sub>2</sub> also facilitate tunnelling. Excess O<sub>2</sub> ions in the insulator act as defects, which release a higher number of electrons as the induced electric field increases. An O<sub>2</sub> deficient insulator contains traps where trap assisted tunnelling takes place and electrons tunnel or hop from one trap to another. A disadvantage of insulators with excess of O<sub>2</sub> is that the films are highly stressed and thus delaminate after a period of time. Substrate B (1:2) exhibits the least amount of current output which suggests that the balanced stoichiometry of the insulator does not favour any kind of trap assisted tunnelling and the current observed is purely due to thermionic and F-N tunnelling. The insulator fabricated with O<sub>2</sub> deficiencies is least stressed and physically more stable.

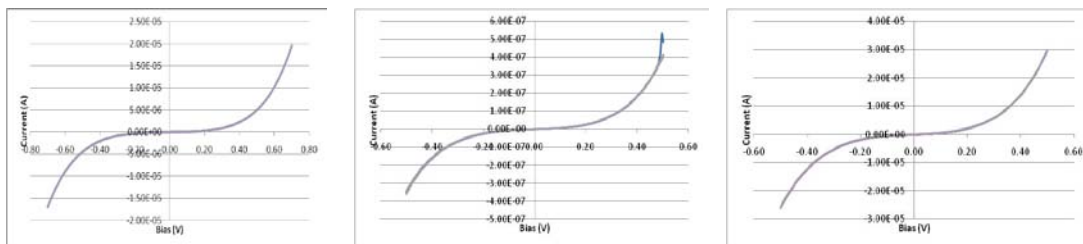


**Figure 7: I-V characteristics of MIM junctions fabricated with different insulator gas ratio, (a) 1:1, (b) 1:2, and (c) 1:3**

**(c) Evaluation of reliable nanomanufacturing of tunnel junction**

Ni/NiO/Cr MIM tunnel junctions with various structures namely, stacked, stepped self-aligned, stepped manual aligned and stepped spacer, were fabricated. Their dc electrical responses were analyzed to identify the effects of diode design on asymmetry and emission current. It was found that the stepped structure with an oxide spacer prevented shorting at the step thus circumventing premature breakdown as exhibited by the other structures. These structures demonstrated better asymmetry and a high enough emission current alleviating the issues caused by the other structures. It was also observed that the current density of the self aligned stepped structure showed less variance across devices than the stepped spacer structure.

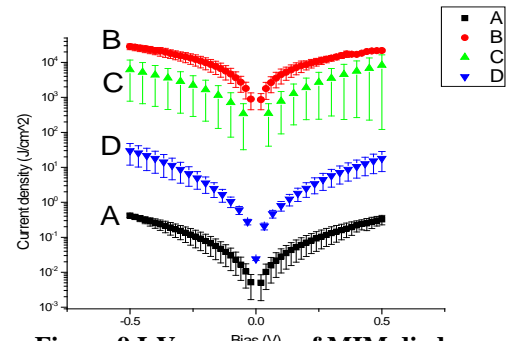


**Figure 9 I-V responses of MIM diodes with stacked structure (A), Self aligned (B), Manually aligned(C) and spaced (D)**

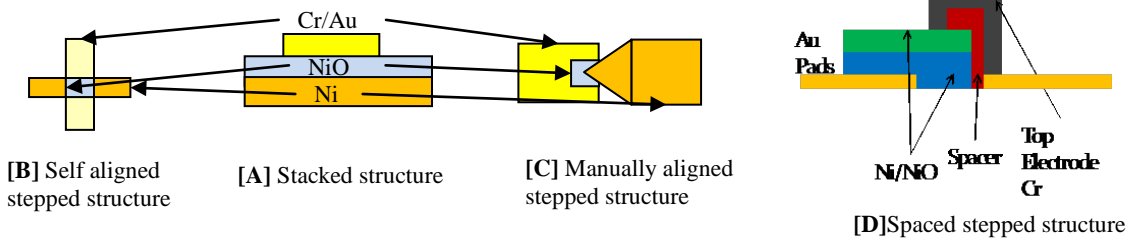


**Figure 8: Different configurations of MIM structure used for evaluating the nanomanufacturability**

**(d) Power Estimation and development of High frequency antenna**

Previously a 94 GHz slot antenna was designed and fabricated. In order to develop a THz antenna, design and simulation needs to be performed using HFSS. As a preliminary step, the 94 GHz antenna was optimized with a dipole fed slot configuration. The return loss of the antenna was determined to be -36dB as shown in Fig 9. The antenna also exhibited a 7 GHz bandwidth at -10dB. The radiation pattern was determined to be a bi-directional donut shaped, with high gain and directivity. The output power generated by the antenna was also determined to be 0.3mW (0.125V) This is the input bias voltage that would be fed to the tunnel junctions by one antenna.

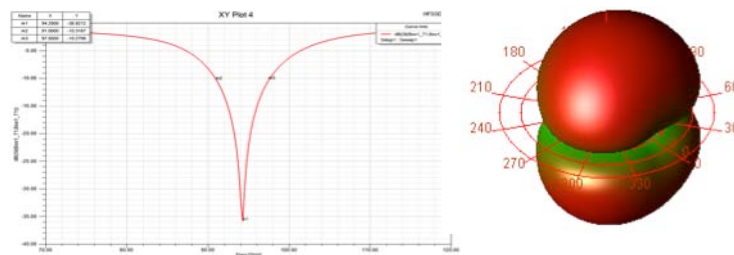


**Figure 9: Plot showing the return loss of the antenna centered at 94 GHz and its radiation pattern**

**Ongoing and Future tasks**

Based on the above accomplishments, the MIM junctions are currently being investigated with organic and inorganic insulators. The organic insulator has the potential to yield higher current, however research is underway to characterize the organic layer to be reliable and reproducible. The robustness of this hybrid stack will be measured and then integrated with the antenna. Similarly, the nanomanufacturability

task, gave an insight into the most favorable design configuration as well as the insulator deposition parameter to be used to develop a reliable device. Based on these experiments, the tunnel junctions will be scaled up in operation frequency and the tunnel junctions will be tested for rectification behavior. Simultaneously, the redesign antenna is being investigated using array concept to improve the power to be inputted into the tunnel junction. This array will be characterized and then used for tunnel junction integration.

### Journal Publications:

1. S. Krishnan, S. Bhansali, E. Stefanakos, Y. Goswami, “*Thin Film Metal-Insulator-Metal Junction for Millimeter Wave detection*,” *Procedia Chemistry* 1, 2009 409-412.
2. S. Krishnan, Y. Emirov, E. Stefanakos, Y. Goswami, S. Bhansali, “*Thermal Stability Analysis of Thin-film Ni-NiOx-Cr Tunnel Junctions*”, *Thin Solid Films*, 515, 2010, 3367-3372.
3. M. Celestin, S. Krishnan, Y. Goswami, E. Stefanakos, S. Bhansali, “*Tunnel Diodes Fabricated For Rectenna Applications Using Self-Assembled Nanodielectrics*”, Accepted for *Procedia Engineering*, 2010.
4. R. Ratnadurai, S. Krishnan, Y. Goswami, E. Stefanakos, S. Bhansali, “*Effects of Dielectric Deposition on the Electrical Characteristics of MIM Tunnel Junctions*”, Accepted for *Procedia Engineering*, 2010.
5. R. Ratnadurai, S. Krishnan, Y. Goswami, E. Stefanakos, S. Bhansali, “*Tunneling characteristics of MIM junctions with change in insulator oxygen concentration* “ Accepted for *Proceedings of AIP*, 2010.

### Conference Presentation:

1. M. Celestin, S. Krishnan, Y. Goswami, E. Stefanakos, S. Bhansali, “*Tunnel Diodes Fabricated using Self-Assembled Alkanethiol Film on Au*,” 2<sup>nd</sup> Annual Research Day, Tampa, FL, 2009.
2. R. Ratnadurai, S. Krishnan, Y. Goswami, E. Stefanakos, S. Bhansali, “*Thin Films based MIM diodes for Infrared Energy Conversion*,” 2<sup>nd</sup> Annual Research Day, Tampa, FL, 2009.
3. S. Krishnan, S. Bhansali, E. Stefanakos, Y. Goswami, “*Thin Film Metal-Insulator-Metal Junction for Millimeter Wave detection*,” *Euroensors XXIII*, Lausanne, Switzerland, 2009.
4. R. Ratnadurai, S. Krishnan, S. Bhansali, E. Stefanakos, Y. Goswami “*Statistical Analysis of Factors affecting the Performance of MIM Tunnel Junctions*,” 217<sup>th</sup> ECS meeting, Vancouver, Canada, 2010.
5. J. Boone, S. Krishnan, S. Bhansali, T. Weller, Y. Goswami, E. Stefanakos, “*Design and Simulation of a Scalable Dipole-fed Slot Antenna*” *WAMICON 2010*, Melbourne Beach, FL, 2010.
6. M. Celestin, P. Campbell, D. Peters, F. McCormick, S. Wix, S. Bhansali, Y. Goswami, S. Krishnan, “*Fabrication and Modeling of Organic Dielectric Tunnel Diodes*,” National Institute for Nano Engineering (NINE), Sandia National Lab, 2010.
7. M. Celestin, S. Krishnan, Y. Goswami, E. Stefanakos, S. Bhansali, “*Tunnel Diodes Fabricated For Rectenna Applications Using Self-Assembled Nanodielectrics*”, *Euroensors XXIV*, Linz, Austria, 2010.
8. R. Ratnadurai, S. Krishnan, Y. Goswami, E. Stefanakos, S. Bhansali, “*Effects of Dielectric Deposition on the Electrical Characteristics of MIM Tunnel Junctions*”, *Euroensors XXIV*, Linz, Austria, 2010.
9. S. Bhansali, “*Next Generation Energy Conversion System Using Antenna Coupled Tunnel Junction*,” *PEFM-2010*, Bhabha Atomic Research Center, India, 2010. (INVITED TALK)

### Patent

1. Sarehraz, M., Buckle, K., Stefanakos, E., Weller, T, and Goswami, Y. “High Frequency Feed Structure Antenna Apparatus and Method of Use” US Patent Number 7,486,236 B2, February 3, 2009.
2. Sarehraz, M., Buckle, K., Stefanakos, E., Weller, T., and Goswami, D.Y., “Dual-Polarized Feed Antenna Apparatus and Method of Use” US Patent 7,619,570 B1, November 17, 2009.
3. Goswami, D.Y., Stefanakos, E., Bhansali, S. “Rectenna Solar Energy Harvester” Provisional Patent Application 12/436,601, May 2009.